



Figure 3-24. View looking northeast from Site 8.



Figure 3-25. Damaged roof at Site 8.

### 3.3.9 Summary of Results

Table 3-2 summarizes the topographic evaluation for the eight subject sites, including the effective wind speed calculated with the  $K_{zt}$  factor.

Table 3-2. Summary of  $K_{zt}$  Calculations.

ID	Wind direction	Feature	$K_1$	$K_2$	$K_3$	$K_{zt}$	Estimated wind speed (mph)	Effective wind speed (mph)
1	WNW	2D escarpment	0.032	1.0	0.939	1.00*	146	146
2	WNW	3D axisymmetrical hill	0.247	-0.866	0.946	1.00	146	146
3	NW	3D axisymmetrical hill	0.495	0.192	0.986	1.20	150	164
4	NW	3D axisymmetrical hill	0.539	0.298	0.978	1.34	150	174
5	E	3D axisymmetrical hill	0.356	-0.047	0.795	1.00	149	149
6	NW	2D escarpment	0.607	0.459	0.919	1.58	149	187
7	NW	3D axisymmetrical hill	0.075	1.00	0.987	1.00*	149	149
8	NE	2D ridge	0.356	1.00	0.975	1.82	149	201

\* $K_{zt}$  modified to 1.00 because slope of hill ( $H/L_H$ ) is less than 0.20.

## 3.4 EXERCISE ON FAILED METAL CONNECTORS AT SITE 6

### 3.4.1 Summary

Failed metal roof connectors were observed at Sites 5 and 6. A limited exercise to back-calculate the wind speed based on this one observed failure is presented here. The failure at Site 6 suggests that the metal connector had an expected ultimate resistance of approximately 3,000 lb. The approximate tributary area of the metal connector is 50 sq ft. For the monoslope roof and estimated wind speed of 149 mph, the uplift force is 3,550 lb, which exceeds the expected ultimate resistance. The rest of this section gives details of the exercise.

### 3.4.2 Verification of Wind Speeds Using Observed Damage

There is large uncertainty in the wind speed estimates because most of the damaged structure was not found or was buried in debris piles, making initial failure locations uncertain. The primary failure mode, however, appears to be a tension failure through the cross section of a metal mechanical connector (Figure 3-19).

Common framing methods for wood-framed structures are used throughout the home building industry, but they can vary based on housing styles, local practices, the contractor performing the work, the materials used, and for other reasons. These variations add significantly to the uncertainty in how any particular failure occurred; however, in the analysis of this site, the likely framing method is evident in the damage, and this assumed framing method is used to determine the likely wind speed that caused the observed damage.

Figure 3-18 shows the valley and the water from which the hurricane winds traveled to this site. The wind direction (from the northwest) was determined by treefall and tree bending evident at the site. From this direction, the wind would have traveled over the roof parallel to the ridge.

### 3.4.3 Roof Framing System

It appeared that the roof was flat on the south side and sloped on the north side. The sloped roof was supported by a beam that was cracked in two places horizontally, parallel to the grain, indicating significant uplift load on the beam. The roof rafters supported by the beam appeared to be 3 ft on center.

### 3.4.4 Failure Mode

The failure used as a proxy for the uplift load on the roof is a torn metal connector indicating a tension failure of the connector (Figure 3-19). The connector is marked as a Simpson Strong-Tie MTS20. The nominal capacity of this connector in uplift according to Simpson Strong-Tie literature is 1,000 lb if installed in Douglas fir lumber and 860 lb if installed in spruce-pine-fir framing lumber (ICC Evaluation Service 2018). Typically, the ultimate load for these connectors is three

times the nominal capacity, so the ultimate load in tension is approximately 2,580 lb to 3,000 lb.

### 3.4.5 Determination of Failure Wind Speed

ASCE 7-16 Equations 27.3-1 and 30.3-1 are used to back-calculate the wind speed required to create the load observed in the failure (Table 3-3).

The estimated wind speed at the site based on the topographical analysis is 187 mph (Table 3-2). This clearly exceeds the minimum required failure speed from Table 3-3. It is not possible to determine a more precise wind uplift speed without more information on the building design and a study of the various material failures, neither of which is available.

Given the limited wind hazard data used and the general assumptions of the structural system, this limited exercise to determine wind speed based on observed failure of one component could suggest the reason for the failure. A forensic study would need more data; this is a limited exercise given the scope and duration of the post-disaster assessment. The exercise was also conducted using a method being developed for a new engineering standard on tornado wind speed estimation using probability theory. Because the method uses the ASCE 7 wind design process as the basis, it is also useful to use in failure analysis for hurricanes. This method has not been balloted for the new standard yet, and has only been peer reviewed within a small task group of the Forensics Task Committee of the standards group; however, that analysis (included as Appendix B) suggests that the wind speed required to have the probability of failure exceed 50% (meaning failure is just as likely as not) is 160 mph. This is much closer to the estimated wind speed at the site, which includes the wind speed-up effect of topography of 187 mph, and significantly higher than the 139 mi/h wind speed for failure estimated using the deterministic method, that is, ASCE 7's wind design method altered to back-calculate a wind speed from a failure load.

*Table 3-3. Possible Wind Speeds at Site 6 Failure Based on Tributary Area and Loading Method.*

<i>Condition</i>	<i>Field of roof 10 sq ft EWA</i>	<i>Field of roof 100 sq ft EWA</i>	<i>Edge of roof 100 sq ft EWA</i>
MWFRS Gable roof w/ $\theta < 7^\circ$	139 mph		
C&C Gable roof w/ $\theta < 7^\circ$	132 mph	132 mph	98 mph

*Notes:*

MWFRS = Main wind force resisting system;

C&C = Component and cladding;

$\theta$  = Slope of roof with respect to the horizontal;

EWA = Effective wind area.

### 3.5 SUMMARY

The following summarizes the information gathered in the topographic effects study at the eight subject sites affected by Hurricane Irma.

- Topographic influences on wind speed can affect structures sited at the tops of hills, ridges, or escarpments.
- For this study, wind speed-up effects are greater for 2D ridges than the other two features described in ASCE 7.
- Terrain features are difficult to classify per the ASCE 7-16 definitions. For this study, specific definitions were determined for 2D ridges and escarpments, leaving 3D axisymmetrical hills to be the default. These terrain features can be very complicated and may not be adequately addressed by calculation using parameters not easily described.
- ASCE 7-16 does not comment on topographic effects on wind speed in a valley where wind is being compressed between two uphill features on either side.

### 3.6 RECOMMENDATIONS

The team has developed the following recommendations for the ASCE 7 standard.

- Improve the terrain feature definitions by expanding the 2D ridge and escarpment definitions and include a definition of a 3D axisymmetrical hill. Illustrations used in the 2015 International Residential Code (shown in Appendix C) might improve the clarity of the descriptions.
- The two primary factors for the magnitude of  $K_{zt}$  are the slope of the hill and the distance of the site of interest from the crest. Consider methods that take into account just these two factors to simplify the results and the understanding by the practice.
- Develop a methodology for calculating wind speed-up effects in a valley.
- Remove the table of topographic multipliers from Figure 26.8-1 in ASCE 7 that are used for only Exposure C. Using the formulas that are a part of this figure provides the same answers, and the information as presented suggests two different methods, which is confusing and incorrect.
- Develop wind-speed maps for topographically complex regions that provide wind speeds including the effects of topography, as was done for Hawaii in ASCE 7-16.

This page intentionally left blank

# CHAPTER 4

## Solar Panel Arrays

The investigation team collected information on solar panel arrays to evaluate the design criteria in ASCE 7. In this chapter,

- Section 4.1 provides an overview of the solar array provisions in ASCE 7.
- Section 4.2 provides observations of rooftop and ground-mounted solar arrays.
- Section 4.3 summarizes the solar array observations.
- Section 4.4 presents solar array recommendations.

### 4.1 ASCE 7 PROVISIONS

Rooftop solar array provisions were incorporated into the 2016 edition of ASCE 7. There are provisions for arrays on low-slope roofs, and for arrays on steep-slope roofs (provided that the panels are generally parallel to the roof surface). Ground-mounted solar arrays are not currently addressed.

ASCE 7-16 defines *solar array* as “any number of rooftop solar panels grouped closely together.” *Rooftop solar panel* is defined as “a device to receive solar radiation and convert it into electricity or heat energy.” Solar panels that produce electricity are also known as PV panels. Solar panel systems that produce hot water are also known as solar hot water heaters.

### 4.2 OBSERVATIONS

#### 4.2.1 Rooftop Solar Array Observations

The team noticed many rooftop PV arrays, but rooftop access was only gained at one building. A few solar hot water heaters were also observed. Residential and non-residential buildings were observed. Roof slopes included steep- and low-slope, and arrays ranged from just a few to a very large number of panels.

None of the observed arrays had wind deflectors. Ballasted solar panels, flexible PV modules [building-integrated PV(BIPV)] installed directly to the roof surface), and PV shingles were not observed.

PV panel wind performance was highly variable. Some arrays had no apparent damage, while others experienced blow-off of many panels and/or panels that were damaged by wind-borne debris.

FEMA USVI RA-5 (2018c) provides an overview of codes, standards, and design guidelines, as well as recommended best practices for attachment design, installation, and maintenance of rooftop solar panels on new and existing buildings. It also provides recommendations for preparations prior to hurricane landfall, and recommendations after a hurricane. It also lists several different factors that can influence wind performance of PV arrays.

Figures 4-1 to 4-11 show the observed rooftop solar arrays.

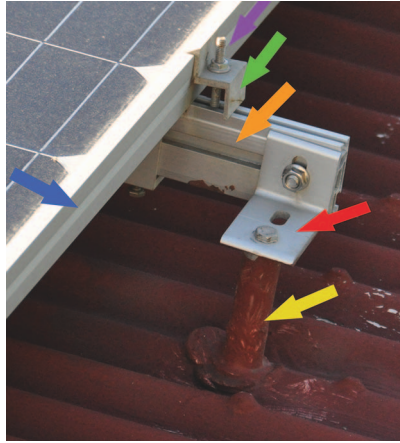
Figure 4-1 shows the roof of one of the observed buildings. Several panels had detached from the rails on one side of the roof. On the other side, all the panels remained attached. These arrays were installed over a corrugated metal roof (a very common roof covering on St. Thomas).

Figure 4-2 shows connection details; they are representative of connections that were commonly observed. The panels were attached with clips that were attached to extruded aluminum rails.

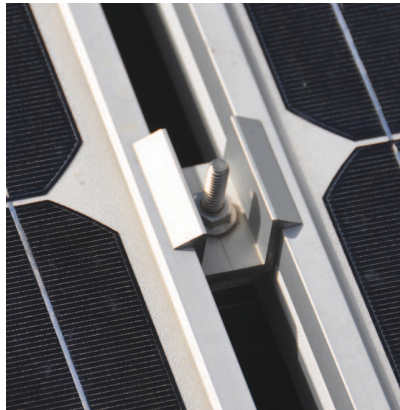
Figure 4-2 shows an end clip, and Figures 4-3 and 4-4 show panel-to-panel clips. The clips were attached to the rails with stainless steel T-bolts with a single nut. The underside of the investigated nuts had a flange that was serrated (the serrations are intended to prevent loosening). The rails were attached to the roof support structure and/or the roof deck with posts (support stands). Figure 4-5 shows another view of the solar hot water heater shown in Figure 4-1.



Figure 4-1. Rooftop solar panels detached from the rails. The yellow line indicates where 14 panels detached. Four of the detached panels (yellow arrows) remained on the roof. See Figure 4-2 for a close-up of the connection details indicated by the yellow circle. The red arrow indicates a component of a solar hot water heater shown in Figure 4-5.



*Figure 4-2. Solar panel array component connections. The blue arrow indicates a panel's extruded aluminum frame. The green arrow indicates a panel end clip. The purple arrow indicates a T-bolt. The orange arrow indicates a rail. The red arrow indicates a clip angle that connects the rail to the post (yellow arrow), which is anchored to the roof structure and/or deck.*



*Figure 4-3. Panel-to-panel clip and T-bolt.*

Figures 4-6 to 4-11 show a building with solar arrays attached to standing seam metal roofs (this building is discussed in Section 3.3.7). The solar panels were attached to rails that were attached to the metal panels with external seam clamps. All or most of the metal roof panels blew off one side of the building (Figure 4-6). Solar panels were attached to those roof panels. Some of the wind-borne roof panel / solar panel debris blew approximately 200 ft. The way the solar panels were attached to the roof panels likely was the direct or contributing cause of roof panel blow-off, as discussed as follows.



Figure 4-4. Panel-to-panel clip and T-bolt that detached from a rail.

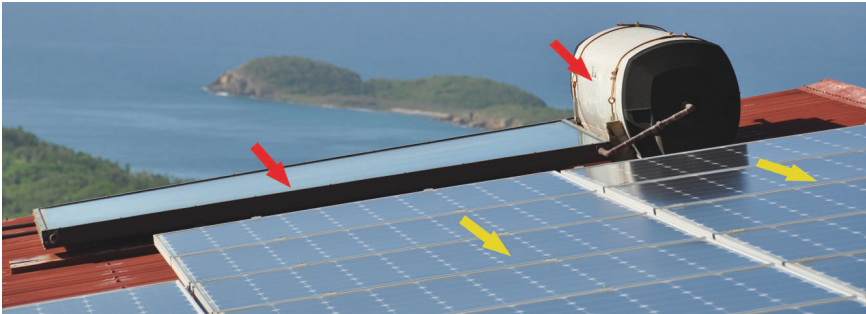


Figure 4-5. Solar hot water heater (red arrows) and PV panels (yellow arrows), also shown in Figure 4-1.



Figure 4-6. Solar panels and metal roof panels blown off the windward roof. The yellow arrows show the extent of the blown-off roof panels. The red arrows indicate metal roof panel and solar panel wind-borne debris.